Plant Physiol. (1994) 104: 17–27

The Use of Fluorescent Tracers to Characterize the Post-Phloem Transport Pathway in Maternal Tissues of Developing Wheat Grains[1]

Ning Wang[2] and Donald B. Fisher[3]*

Department of Botany, Washington State University, Pullman, Washington 99164–4238

Various polar fluorescent tracers were used to characterize the pathways for apoplastic and symplastic transport in the "crease tissues" (i.e. the vascular strand, chalaza, nucellus, and adjacent pericarp) of developing wheat (*Triticum aestivum* L.) grains. With mostly minor exceptions, the results strongly support existing views of phloem unloading and post-phloem transport pathways in the crease. Apoplastic movement of Lucifer yellow CH (LYCH) from the endosperm cavity into the crease was virtually blocked in the chalazal cell walls before reaching the vascular tissue. However, LYCH could move slowly along the cell wall pathway from the chalaza into the vascular parenchyma. Slow uptake of LYCH into nucellar cell cytoplasm was observed, but no subsequent symplastic movement occurred. Carboxyfluorescein (CF) imported into attached grains moved symplastically from the phloem across the chalaza and into the nucellus, but was not released from the nucellus. In addition, CF moved in the opposite direction (nucellus to vascular parenchyma) in attached grains. Thus, the post-phloem symplastic pathway can accommodate bidirectional transport even when there is an intense net assimilate flux in one direction. When fresh sections of the crease were placed in fluorochrome solutions (e.g. LYCH or pyrene trisulfonate), dye was rapidly absorbed into intact cells, apparently via unsealed plasmodesmata. Uptake was not visibly reduced by cold or by respiratory inhibitors, but was greatly reduced by plasmolysis. Once absorbed, the dye moved intercellularly via the symplast. Based on this finding, a size-graded series of fluorescein-labeled dextrans was used to estimate the size-exclusion limits (SEL) for the post-phloem symplastic pathway. In most, and perhaps all, cells of the crease tissues except for the pericarp, the molecular diameter for the SEL was about 6.2 nm. The SEL in much of the vascular parenchyma may be smaller, but it is still at least 3.6 nm. Channel diameters would likely be about 1 nm larger, or about 4.5 to 7.0 nm in the vascular parenchyma and 7.0 nm elsewhere. These dimensions are substantially larger than those for "conventional" symplastic connections (about 3 nm), and would have a greater than proportionate effect on the per channel diffusive and hydraulic conductivities of the pathway. Thus, relatively small and probably ultrastructurally undetectable adjustments in plasmodesmatal structure may be sufficient to account for assimilate flux through the crease symplast.

Based on the constancy of assimilate import into developing wheat (*Triticum aestivum* L.) grains over a wide range of cavity sap osmolalities and Suc concentrations, we have concluded that the rate of import must be controlled by transport processes in the maternal tissues of the grain (Wang and Fisher, 1994). Wolswinkel (1992), as well, has expressed a similar view, citing the capacity of empty legume seed coats and maize pedicels (Porter et al., 1985) to sustain in vivo transport rates in the absence of embryonic tissues. Jenner (1985a) also has suggested that the growth rate of wheat grains is controlled by transport processes within the maternal tissues. To understand these processes, it is important to characterize clearly the transport pathways there.

Jenner (1985a, 1985b) has emphasized two anatomical regions of likely importance in assimilate import into wheat grains. One is the phloem pathway at the base of the grain, where a discontinuity in the xylem (Zee and O'Brien, 1970a) results in a substantial degree of independence of grain water relations from the rest of the plant (Barlow et al., 1983; Fisher, 1985). The other region is the post-phloem pathway across the "crease tissues" (i.e. the vascular strand, chalaza, nucellus, and adjacent pericarp). With respect to the latter pathway, Jenner (1974) noted the sharply declining Suc concentration along it and suggested that diffusion could account for transport from the phloem to the endosperm cavity. This view receives strong circumstantial support from the fact that most of the increase in grain dry weight occurs without an increase in water content (Sofield et al., 1977), suggesting that assimilates move across the crease independently of water.

Diffusion may, in fact, provide an adequate explanation for assimilate transport across the crease tissues. However, as the following considerations indicate, the process may be more complex than this. The first consideration is the adequacy of diffusion as a basis for transport across the crease. Suc concentrations in the crease phloem and in the endo-

[1] This work was supported by a grant from the National Science Foundation (DCB-9019411).

[2] Present address: Laboratory of Biomedical and Environmental Sciences, University of California, Los Angeles, 900 Veteran Avenue, Los Angeles, California 90024–1786.

[3] Address through July 1994: Department of Cellular and Environmental Physiology, Scottish Crop Research Institute, Invergowrie, Dundee DD2 5DA, UK; fax 44–382–562426.

* Corresponding author; fax 1–509–335–3517.

Abbreviations: CF, 5(6)-carboxyfluorescein; CFDA, 5(6)-carboxyfluorescein diacetate; F-dextran, fluorescein-dextran; LYCH, Lucifer yellow CH; mOsm, milliosmolal; PTS, 8-hydroxy-1,3,6-pyrenetrisulfonate; R_g, radius of gyration; R_h, hydrodynamic, or Stokes, radius; SEL, size exclusion limit.

sperm cavity, about 400 μm apart, are about 600 and 75 mM, respectively (Fisher and Gifford, 1986; Fisher and Wang, 1993; Wang and Fisher, 1994). Given the diffusion coefficient of Suc (5.2×10^{-10} m^2 s^{-1}) and ignoring barriers to diffusion, a linear gradient between the two would sustain a Suc flux density of 6.8×10^{-4} mol m^{-2} s^{-1}. The actual flux density in the chalaza, based on a Suc import rate of 220 nmol h^{-1} (Fisher and Wang, 1993), is 6.5×10^{-5} mol m^{-2} s^{-1}. Clearly, however, diffusion along this pathway will be significantly hindered. Symplastic transport is limited by cell-to-cell movement, not by transcellular movement (Barclay et al., 1982; Tucker et al., 1989). Since there are about 15 cells between the sieve tubes and the endosperm cavity, there would be a cell-to-cell Suc gradient (assuming equal steps) of 35 mM at each step. Goodwin et al. (1990) have measured a permeability coefficient of 1.1×10^{-6} m s^{-1} for intercellular CF movement in *Egeria* leaves, and the data of Tucker et al. (1989) for CF movement in *Setcreasea* stamen hairs provide a similar value of 0.8×10^{-6} m s^{-1}. Assuming a permeability coefficient of 1×10^{-6} m s^{-1}, the calculated average Suc flux density in the crease would be 3.5×10^{-5} mol m^{-2} s^{-1}, reasonably close to the actual flux density. For most of the post-phloem pathway, however, the actual cell-to-cell Suc gradient would be appreciably less than 35 mM per cell. The highest concentration in the vascular parenchyma is estimated to be 300 mM, with much of the remaining gradient apparently occurring across only two or three vascular parenchyma cells adjacent to the chalaza (Fisher and Wang, 1993). In the rest of the vascular parenchyma, and in the chalaza and nucellus, the Suc gradient could only be a fraction of the 35 mM per cell assumed above. Although such calculations are clearly imprecise at present, they cast doubts on the adequacy of diffusion as the sole basis for post-phloem transport across the crease.

Although steep concentration gradients will clearly contribute to diffusive movement along the symplast, they will almost certainly give rise to turgor gradients as well. This, in turn, raises questions about the extent to which bulk flow might contribute to movement. In this context, it is relevant to note that, over longer periods (several hours or more), transport from the phloem to the endosperm cavity must be a nonselective process, a characteristic of bulk flow; all assimilates imported via the phloem move to the endosperm cavity. Conceivably, even transmembrane movement through the nucellar membranes could occur as bulk flow through pores. Finally, even if osmotic and pressure gradients along the cell-to-cell pathway were balanced to prevent net volume flow, present theories of solute and water movement within small pores (e.g. 2 to 4 times the solute diameter) predict an oppositely moving coaxial flow pattern within the pore rather than simple interdiffusion of solutes and water (Anderson and Malone, 1974; Finkelstein, 1987). Especially at these dimensions, patterns of diffusive and convective movement are crucially dependent on channel size.

The initial purpose of this research was to identify potential pathways of apoplastic and symplastic movement in the crease tissues, to determine the extent to which symplastic movement might be bidirectional, and to determine whether nucellar cell membranes are nonspecifically permeable. However, we also found that strongly polar tracers (e.g. PTS, LYCH) could rapidly enter intact crease cells from a cut surface, apparently via unsealed plasmodesmata. This allowed the use of size-fractionated F-dextrans to estimate the SELs of plasmodesmata in the crease tissues. Knowledge of the SEL is essential not only for calculating the total area for cell-to-cell movement, but also for characterizing mass transport within individual pores.

MATERIALS AND METHODS

Plant Materials and Growth Conditions

Wheat plants (*Triticum aestivum* L. cv SUN 9E) were grown in a growth chamber. Growth conditions were as described in previous publications (Fisher and Wang, 1993). Briefly, plants were grown on a 16-h photoperiod at a PPFD of 450 μmol m^{-2} s^{-1} and a day/night temperature regime of 22/16°C. Plants were irrigated with water at 16-h intervals and with a complete nutrient solution once a week. Ears were tagged at anthesis and used for experiments 14 to 18 d later.

Application of Dye Solutions

Import of CF via the phloem was accomplished by cutting the stem off underwater, just below the flag leaf node, and transferring the cut end of the upper shoot (flag leaf, peduncle, and ear) into 0.1 mM CFDA. The shoot was illuminated with a PPFD of 800 μmol m^{-2} s^{-1} from a water-filtered metal halide lamp. The appearance of CF in sieve tubes was followed by collecting exudate from severed aphid stylets established on the peduncle (Fisher and Frame, 1984). Grains were removed occasionally during the next 40 h to check for the appearance of CF in the crease tissues. Fresh sections were cut 100 μm in thickness with a vibrating microtome and examined by epifluorescence microscopy.

To trace the apoplastic pathway from the endosperm cavity into the crease and to address the possibility of nucellar cell membrane leakiness, 10 mM LYCH in standard 300-mOsm perfusion medium (Wang and Fisher, 1994) was perfused at 12 μL h^{-1} through the cavity of attached grains. Crease tissues were dissected from the grains, rinsed briefly (three times, approximately 2 s each) in perfusion medium without LYCH, quick-frozen, and processed for plastic embedding (described below). We also investigated the effect on apoplastic LYCH movement of increasing the water potential gradient across the crease tissues, normally about 0.3 MPa lower in the pericarp than in the cavity (Fisher, 1985, and additional measurements), to about 1 MPa. This was approached by using a 27-gauge hypodermic needle to scoop away the green outer pericarp layer of the crease region of an excised grain and applying a −1.7-MPa solution of PEG 6000 to the exposed surface of broken cells. For brevity, this will be referred to as "abrasion," although the three to five cell layers removed were more than might be inferred from the term. Dye experiments showed that solute movement through pericarp walls was slow if only the epidermal cells were broken.

Bidirectional symplastic movement across the crease tissues was investigated by CFDA applications. To follow the movement of CF from the nucellus to the vascular parenchyma cells, against the direction of assimilate import, the endosperm cavities of attached grains were perfused with 0.1 mM

CFDA in standard medium. In a separate experiment, the possibility that CFDA perfusion might affect assimilate import was evaluated by measurement of ^{14}C-photosynthate import into similar, CFDA-perfused grains (Wang and Fisher, 1994).

CFDA was applied to the abraded crease of excised grains to follow CF movement in the opposite direction (vascular parenchyma to the nucellus). Two hours after CFDA application, the grains were washed with standard medium for 20 min and fresh cross-sections were cut 100 μm in thickness with a vibrating microtome and examined by epifluorescence microscopy.

The direct uptake of polar fluorescent tracers (LYCH, PTS, F-dextran, etc.) into intact cells was followed by incubating fresh sections, cut on a vibrating microtome, in solutions of the dye in standard medium. Specifics of the treatment conditions are indicated in the text and in figure legends.

F-dextrans were obtained from Molecular Probes, Inc. (Eugene, OR). All other chemicals were from Sigma.

Localization of Tracers in Plastic Sections

To rigorously prevent possible secondary movement of fluorescent tracers and/or to allow subcellular localization, tissue samples were quick-frozen, freeze-substituted in acetone, and embedded in Spurr's resin (Fisher and Housley, 1972). Sections 1 to 4 μm in thickness were cut dry and mounted in immersion oil. To encourage flattening of the section, the volume of oil was kept to a minimum. The fluorescence distribution pattern in the sections was examined by epifluorescence microscopy.

The possible presence in the crease tissues of enzymes that might degrade F-dextran was investigated by grinding the crease tissues from 10 grains (about 20 mg fresh weight) in 20 μL of perfusion medium and incubating the extract with F-dextran 3000 for 1 h at 21°C. As suggested by the supplier (Molecular Probes, Inc.), the extract was spotted on silica gel TLC plates and run in chloroform:methanol:water (70:25:5, v/v) to check for hydrolysis.

Estimation of SELs for Symplastic Movement

Two sizes of F-dextrans, with nominal mol wts of 3,000 and 10,000 (Molecular Probes, Inc.), were fractionated according to the procedures described by Luby-Phelps et al. (1986) and Luby-Phelps (1989) with some modifications. Briefly, Biogel P2 (F-dextran 3,000) or P6 (F-dextran 10,000) was equilibrated with glass-distilled water, loaded into a 3 × 50 cm column, and washed with 5 bed volumes of distilled water. F-dextran in 3 mL of water was loaded onto the column and eluted at 25 mL h^{-1} (F-dextran 3,000) or 9 mL h^{-1} (F-dextran 10,000). Because of the slower rate, the latter separation was run at 4°C and collection was terminated after 62 fractions. Fractions of 1.3 mL were assayed for fluorescence intensity, freeze dried in a speed vacuum concentrator, and stored at −80°C.

The diffusion coefficients of selected F-dextran fractions and other compounds were measured by diffusion into an agar column according to the procedures of Schantz and Lauffer (1962), with minor modifications. NaCl (20 mM) was included in the solutions to minimize interaction between agar gel and F-dextrans, and to conserve F-dextran, the diameter of the agar column was reduced to 1.6 mm. This was accomplished by casting the agar column in a screw-type 0.5-mL syringe, which also provided precise advancement for slicing the gel after the diffusion period. The temperature was 21°C. R_h was calculated from the Stokes-Einstein equation (see Table I, footnote).

Two approaches, both using size-fractionated F-dextrans, were taken to the estimation of SELs for movement through plasmodesmata. One addressed only the uptake and retention of F-dextran by crease tissue cells, whereas the other depended on uptake and cell-to-cell movement. In the first, fresh sections, 100 μm in thickness, were incubated in various-sized F-dextrans (R_h = 0.98–2.6 nm) at 0°C followed by a 15-min wash in standard medium at room temperature. The incubation time was 1 min for the smallest (0.98 nm) F-dextran. Incubation times for larger F-dextrans were prolonged in proportion to their hydrodynamic radius (i.e. in inverse proportion to their diffusion coefficients). Sections from a single grain were used in each experiment. Each experiment was repeated eight times with grains from different plants.

The second approach to SEL estimation examined the cell-to-cell movement of F-dextran along the crease tissue axis. A grain was cut transversely and the cut surface was incubated for 2 min in 5 mM F-dextran at 0°C, followed by a wash in standard medium at room temperature for 28 min. Serial sections, 75 μm thick, were cut with a vibrating microtome, washed at room temperature for 20 min in standard medium, and examined by epifluorescence microscopy.

Fluorescence Photomicroscopy

Sections were examined by epifluorescence microscopy with a Leitz Ortholux II microscope using an H2 filter cube. Color photos were taken with Fuji color film rated at 1600 ASA. Black and white pictures were taken with Kodak T-Max film rated at 400 ASA, and a red-cutoff filter was used to eliminate Chl fluorescence. When comparisons of relative fluorescence intensity were important, the same exposure time was used for each micrograph of the series.

RESULTS

Apoplastic and Symplastic Pathways within the Crease Tissues

Figure 1 illustrates the distribution of LYCH in dry-cut plastic sections of freeze-substituted crease tissues after perfusing the endosperm cavity with LYCH. After 30 min of perfusing an attached grain (Fig. 1A), LYCH had penetrated throughout the thick nucellar cell walls and had begun to move into the thinner walls of the chalaza. (A diagram of the crease tissues is provided in Fig. 2D.) After 1 h, LYCH was present in all cell walls of the chalaza and had begun to move into walls of the vascular parenchyma (Fig. 1B). When the water potential gradient across the crease was increased by applying −1.7 MPa PEG to the abraded crease surface of excised grains, LYCH from the endosperm cavity moved

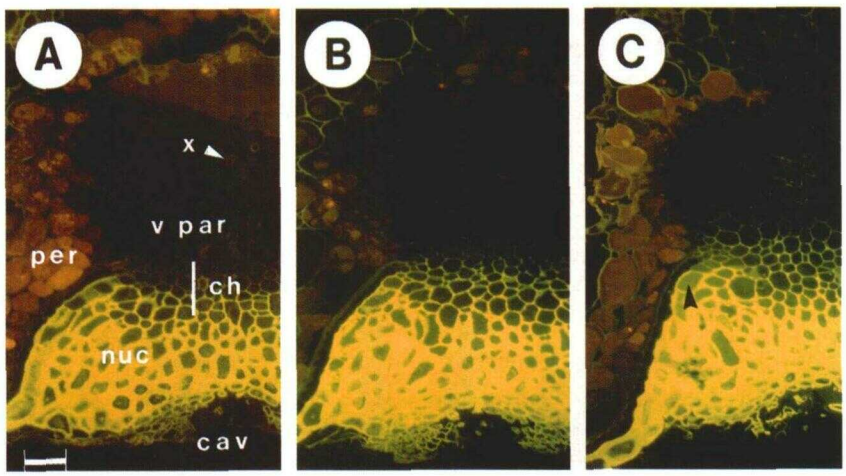

Figure 1. LYCH distribution in the crease tissues of freeze-substituted, plastic-embedded wheat grains after perfusion of the endosperm cavity with 10 mM LYCH in standard medium. Crease tissues were dissected from the grain and rinsed briefly three times (approximately 2 s each) in standard medium before freezing. Sections 4 μm in thickness were cut dry and mounted in immersion oil for examination by epifluorescence microscopy. LYCH fluoresces bright yellow. Some weaker autofluorescence, mainly in the pericarp, is distinguishable by its dull orange color. Bar (lower left) = 50 μm. A, Attached grain, perfused 0.5 h. x, Xylem; v par, vascular parenchyma; ch, chalaza; nuc, nucellus; cav, endosperm cavity; per, pericarp. B, Attached grain, perfused 1 h. C, Excised grain, perfused 1 h. Prior to perfusion, the crease pericarp was abraded and covered with a drop of PEG 6000 (water potential = −1.7 MPa). Uptake of LYCH into a cell of the nucellar epidermis is indicated by the black arrowhead.

somewhat further, penetrating well into walls of the vascular parenchyma after 1 h (Fig. 1C).

Transpirationally absorbed CFDA resulted in the introduction of CF into the phloem, thus allowing visualization of the pathway followed by a polar solute as it entered attached grains normally via the phloem (Fig. 2A; see Fig. 3, "control," for autofluorescence in an unstained section). Strong CF fluorescence was present in peduncle aphid-stylet exudate within 2 h, and continued to be present throughout the experiment. CF was detected in the grain phloem 3 h after CFDA uptake began (not shown) and, except for the pericarp, was present throughout the crease tissues after 12 h (not shown). Except for a strong increase in fluorescence intensity and some movement into the pericarp, no further change had occurred after 40 h (Fig. 2A). In particular, there was no evidence of CF movement into the endosperm cavity or endosperm.

Symplastic movement across the crease tissues, in both directions, could be shown by applying CFDA directly to the grain. Figure 2B shows the presence of CF throughout the crease tissues 2 h after perfusing the cavity of an attached grain with CFDA. (In a separate experiment, CFDA perfusion for 5 h did not affect assimilate movement into the grain; the "relative unloading ratio" was 1.27 ± 0.33 [Wang and Fisher, 1994]). Note that the direction of CF movement from the nucellus to the vascular parenchyma cells would have been against the movement of incoming assimilates. Movement of CF in the opposite direction is shown in Figure 2C, which illustrates the distribution of CF in the crease 2 h after applying CFDA to the abraded crease of an excised grain. Although the outer pericarp and outer cell layer or so of the vascular parenchyma were removed in this experiment (see "Materials and Methods"), a similar CF distribution, at a

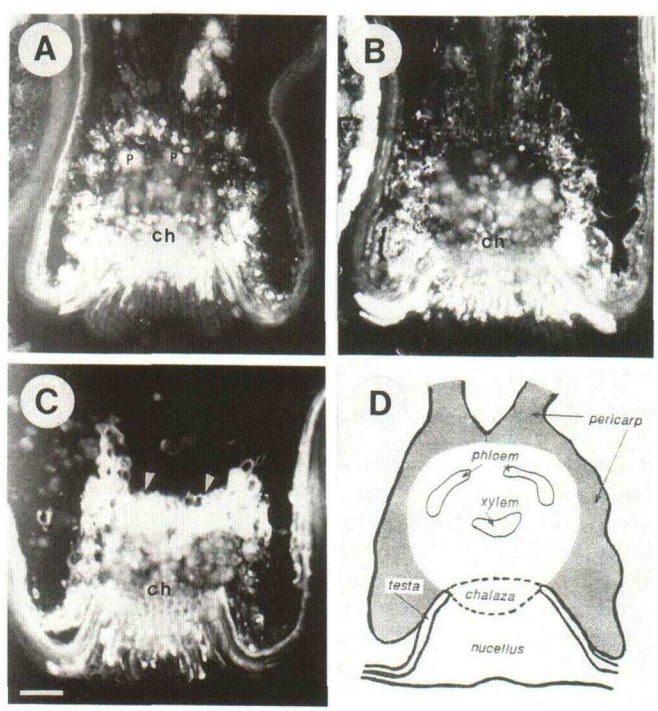

Figure 2. Epifluorescence micrographs showing the distribution of CF in the crease tissues after uptake of CFDA from: the transpiration stream (12-h uptake from the severed penultimate internode) (A); the endosperm cavity of an attached grain (2-h perfusion) (B); and the abraded surface (white arrowheads) of the crease tissues of an excised grain (2-h incubation) (C); ch, chalaza; p, phloem. Bar = 100 μm for all three figures, A through C. D, Diagram of tissues in a cross-section of the crease region of a wheat grain.

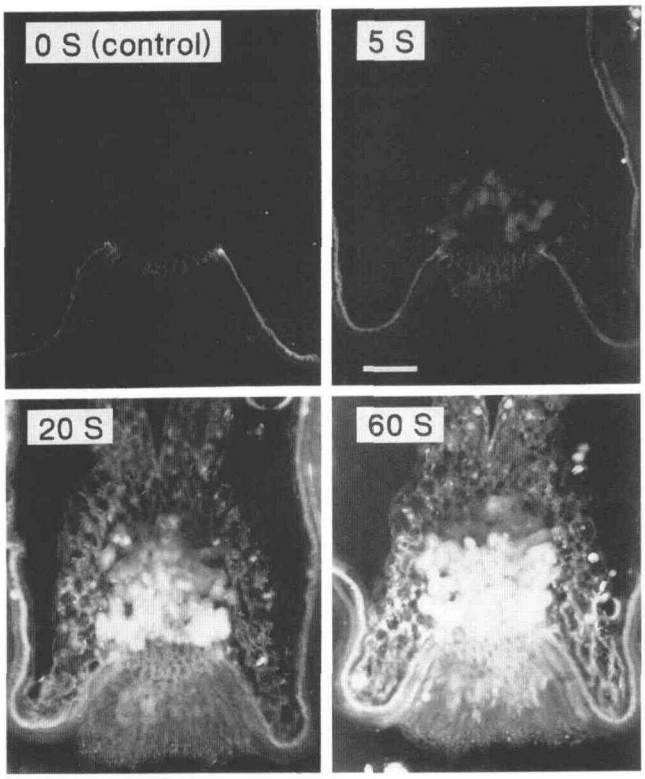

Figure 3. Rapid uptake of LYCH by crease cells. Fresh sections, 100 μm in thickness, were incubated for the times indicated in 0.5 mM LYCH in standard medium, washed for 15 min in standard medium, and examined by epifluorescence microscopy. A moderate amount of autofluorescence is present in the chalaza and in the testa cuticle (control panel). The nucellus and xylem vessels are weakly autofluorescent. Bar = 100 μm.

much-reduced fluorescence intensity, resulted when only the epidermal cells were broken (not shown).

Clear evidence was observed of limited LYCH uptake from the endosperm cavity into the cytoplasm of nucellar cells. This was most apparent in the larger-celled nucellar epidermis (Fig. 1C, arrow), but was also evident in other nucellar cells, including those near the chalaza. (The one to three layers of cells bordering the endosperm cavity are nonliving.) However, the rate of uptake was very slow. In many cells the fluorescence was not strong and, in contrast to the symplastic movement of CF (Fig. 2) and other dyes (next section), there was no further movement of LYCH across the crease.

Perfusion of the endosperm cavity for 1 h with 10 mM sulfosuccinimido biotin, a nonpermeant amino-reactive tracer (Grimes et al., 1988), also resulted in labeling of the cytoplasm and nuclei of nucellar cells but little or no labeling of chalazal cells (not shown).

Symplastic Uptake of Polar Dyes from the Apoplast

Attempts to use fresh sections to investigate some aspects of apoplastic dye movement resulted in irregular observations of apparent uptake of supposedly nonpermeant tracers, notably LYCH and PTS, into intact cells. This prompted a more systematic investigation into the basis for such uptake.

The absorption of polar dyes into intact cells of fresh-sectioned crease tissues occurred with striking rapidity (Fig. 3). Uptake of LYCH was evident after only 5 s of incubation and continued for 1 to 2 min, after which there was no visually discernible increase in fluorescence (not shown).

Uptake of polar tracers was not noticeably reduced by cold or by respiratory inhibitors (not shown; however, see Figs. 4, 8, and 9 for experiments involving uptake at 0°C). At 0°C (i.e on ice), uptake of LYCH by crease cells appeared to be as rapid as at room temperature. Similarly, uptake of LYCH was not substantially reduced by preincubation of fresh sections with 0.3 mM KCN for 5 min or with 0.15 mM CCCP for 20 min at 0°C before a 1-min incubation with LYCH at 0°C. (The experiments with inhibitors were conducted at 0°C to avoid the marked reduction in dye uptake that occurred with preincubation at room temperature; see below.)

The effect of plasmolysis on uptake provided more direct, but still circumstantial, evidence for the involvement of plasmodesmata. Uptake of PTS was strongly inhibited by plasmolyzing fresh sections for 20 min in 1070 mOsm Suc before incubation with PTS (Fig. 4). Cells in plasmolyzed sections remained viable, since they showed strong fluorescence after incubation in CFDA (not shown).

Further evidence that transmembrane movement was not involved in dye uptake comes from the distribution of PTS in fresh sections immediately after a brief (2 min) uptake period. Figure 5 shows the PTS distribution in dry-cut plastic sections of these freeze-substituted fresh sections. Here, PTS entered the cytoplasm of chalazal cells at the cut surface just as rapidly as it entered other cells (Fig. 5B), even though chalazal cell walls, distinguishable by their orange-yellow autofluorescence, excluded PTS. Conversely, many parenchyma cells not at the cut surface but adjacent to PTS-containing xylem vessels showed no PTS uptake. Thus, the condition for PTS entry appears to be the exposure of a cut surface, not just the plasma membrane, to the dye solution.

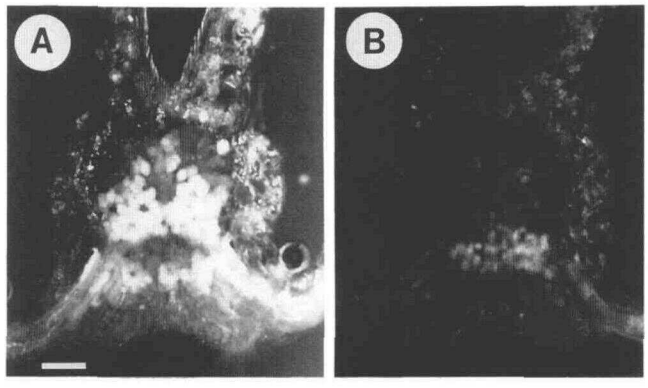

Figure 4. Effect of plasmolysis on PTS uptake. Fresh sections, 100 μm thick, were preincubated for 20 min at 0°C in standard 300-mOsm medium (A) or, to induce plasmolysis, in 1070-mOsm Suc (B). The sections were then transferred to 0.5 mM PTS in the same medium at 0°C for 1 min followed by a 20-min wash in the original solution at room temperature. Bar = 100 μm.

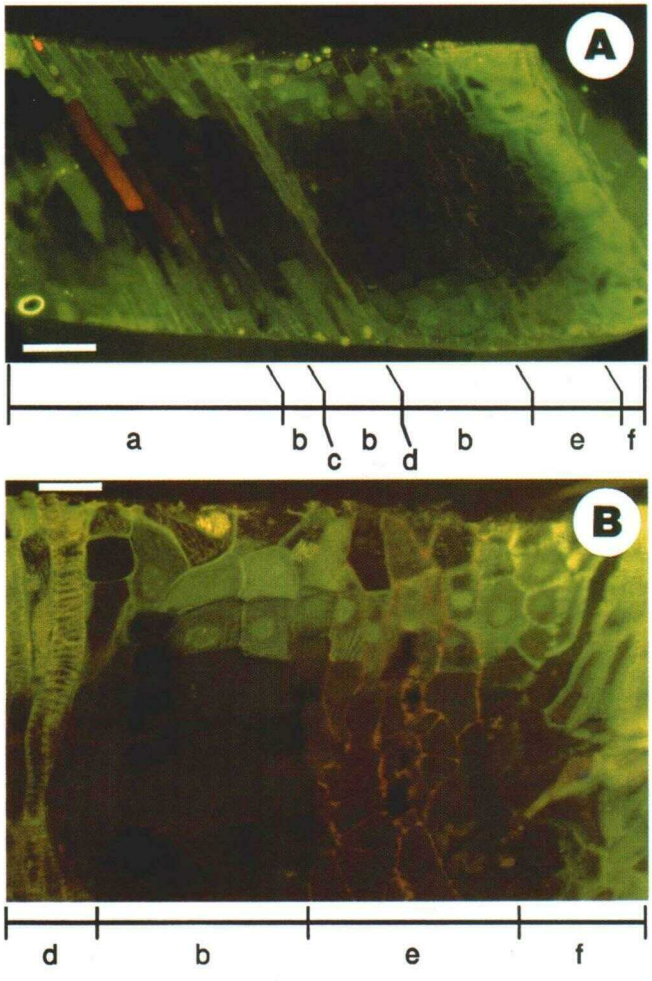

Figure 5. Distribution of PTS in a 400-μm-thick fresh cross-section of the crease after a 2-min incubation in 10 mM PTS in standard medium. The section was frozen immediately (no wash), freeze-substituted in acetone, and embedded in epoxy resin. Dry sections 2.5 μm thick were cut perpendicular to the surface of the original fresh section (i.e. parallel to the grain axis) and the sections were mounted in immersion oil. A, Low magnification, bar = 100 μm; B, higher magnification (different section from A), bar = 30 μm. a, Pericarp; b, vascular parenchyma; c, phloem; d, xylem; e, chalaza; f, nucellus.

Figure 5A shows several additional features of interest in the context of apoplastic and symplastic solute movement. Most importantly, in comparing the PTS distribution in the xylem to that in the vascular parenchyma, it illustrates the limitations imposed by cell-to-cell symplastic transport in the crease. Although sufficient time elapsed for diffusion to reach near-equilibrium along the 400-μm length of xylem, not even traces of PTS were present more than 100 μm into the symplastic pathway. Finally, movement into nucellar cell walls was very rapid, with PTS visible throughout almost all of the thick-walled cells in this tissue after the 2-min uptake period. This contrasts sharply with the much slower subsequent movement of dye in the chalazal walls (Fig. 1).

Some changes with time were noted in dye uptake and cellular distribution (observations not shown). Preincubation of fresh sections in standard medium at room temperature for more than 5 min usually resulted in obviously reduced uptake of LYCH and PTS. At 0°C, however, dye uptake was not noticeably reduced even after 20 min of preincubation. For this reason, preincubation treatments (e.g. plasmolysis, inhibitors) and some uptake treatments were carried out at 0°C.

With longer post-uptake incubation times (tens of minutes), the intracellular distribution of the smaller (i.e. nondextran) dyes often became markedly uneven as a result of accumulation into a subcellular compartment. This was most marked in the nucellus and in vascular parenchyma near the chalaza and accounts for much of the CF fluorescence in the sections shown in Figure 2. In dry-cut plastic sections of freeze-substituted crease tissues, most of the fluorescence was located in small vesicles that could not be positively identified cytologically (observation not shown). The dye had not been simply insolubilized, since all of the fluorescence (PTS, in this case) disappeared on washing the plastic section with water.

After absorption from the apoplast, polar dyes were mobile within the symplast. Figure 6 illustrates the distribution of PTS in the crease of an excised grain 2 h after applying 10 mM PTS to the abraded pericarp. To monitor dye movement into the endosperm cavity, the cavity was perfused with standard medium at 15 μL h^{-1}. Despite the strong accumulation of PTS in the nucellar cells, further movement into the cavity was very limited. Some PTS eventually appeared in the cavity, but the effluent concentration was still less than 1 μM after 2 h. LYCH was not detected in the cavity after 2 h of dye application.

SELs for Cell-to-Cell Movement in the Crease Tissues

The apparent role of plasmodesmata as a pathway for movement into cells from the apoplast provided a basis for

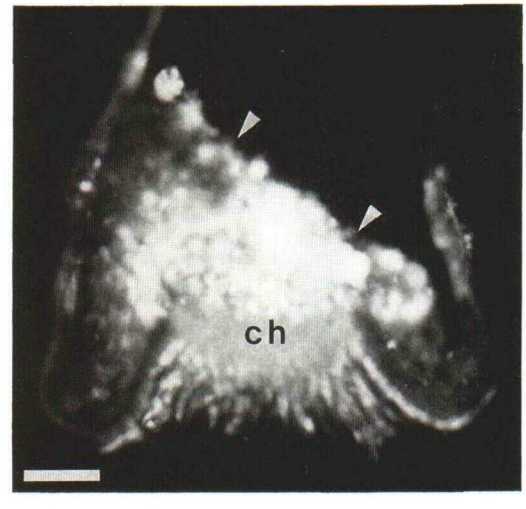

Figure 6. Distribution of PTS in the crease tissues of an excised grain after applying 10 mM PTS in standard medium to the abraded surface of the crease (white arrowheads) for 2 h. The abrasion removed the outer pericarp and some vascular parenchyma cells. The grain was washed for 20 min in standard medium before fresh-sectioning at 100 μm. Sections were washed for an additional 10 min before viewing. ch, Chalaza. Bar = 100 μm.

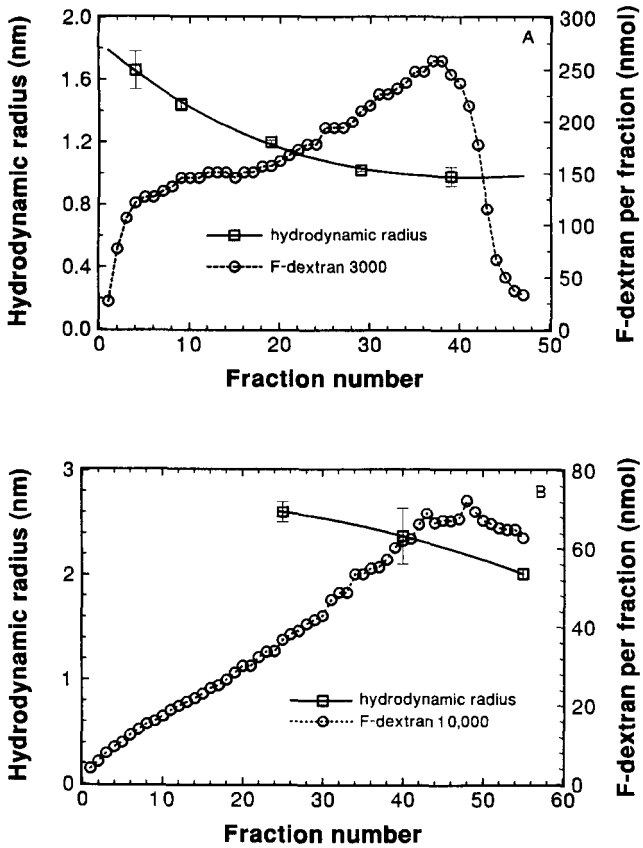

Figure 7. Hydrodynamic (Stokes) radii (R_h) of F-dextran fractions from commercial preparations of nominal M_r = 3,000, separated on a Biogel P2 column (A), and nominal M_r = 10,000, separated on a Biogel P6 column (B). Fraction numbers commence with the initial appearance of F-dextran in the column effluent. Hydrodynamic radii were calculated from measurements of diffusion coefficients.

estimating the SEL for symplastic transport within the crease tissues. Initially, several dye-peptide complexes were synthesized as size probes. However, it became apparent that the SEL range was quite substantial, making it desirable to employ a more regularly graded series of chemically similar probes for this work.

A continuous size range of fluorescein-labeled dextrans was generated by fractionating commercially available preparations on Biogel columns (Fig. 7). The hydrodynamic radii of fractionated F-dextran 3,000 (Fig. 7A) and F-dextran 10,000 (Fig. 7B) used in our SEL experiments ranged from 0.98 to 2.6 nm. The SD for R_h (indicated by error bars for each point; two or four measurements for each fraction) was less than ±8% for all but one fraction, where it was ±11%. The accuracy of the method was verified with Suc (single determination), which yielded a diffusion coefficient indistinguishable from the literature value (Table I). Where data are available, our values for diffusion coefficients compare favorably with existing measurements and estimates (Table I). Minor differences for the dextrans are most likely due to differences in mol wts rather than to error in diffusion measurements.

We found no evidence that F-dextran might be degraded in the crease tissues. Incubation with crease tissue extract did not alter its TLC mobility. Once absorbed, F-dextran retained its uniform distribution within cells (Figs. 8 and 9), with no indication of the progressive compartmentation that characterized the smaller dyes. Movement within the crease tissue symplast was clearly dependent on the size of the applied F-dextran (see below).

As in the case of smaller dyes, F-dextrans were mobile in the symplast after their initial uptake into intact cells. Figure 8 shows the movement of different-sized F-dextrans along the grain axis after a brief exposure of the surface of a transverse cut to dye solution, followed by a wash with dye-free medium for 28 min. (Note that, except for the pericarp, there are no intercellular spaces in the crease tissues, so the possibility of movement by this path is mostly eliminated.) All three sizes of F-dextran (0.98, 1.41, and 2.00 nm) entered all cell types at the crease surface except for the pericarp, and

Table I. *Measured values of diffusion coefficients and comparisons with reported values*

Compound (M_r)	Diffusion Coefficient		R_h[a]	Reference
	Measured	Reported		
	$m^2\ s^{-1} \times 10^{10}$ (21 °C)		nm	
Suc (M_r = 342)	4.7	4.7	0.47	Lide, 1990
CF (M_r = 374)	3.63 ± 0.04[b]	3.61[c]	0.61	Barclay et al., 1982
LYCH (M_r = 443)	3.24 ± 0.05[b]		0.68	None found
F-dextran (M_r = 3,000)	1.98[d]	1.83[e]	1.11	Paine et al., 1975
F-dextran (M_r = 10,000)	0.89[d]	0.94	2.47	Granath and Kvist, 1967

[a] Calculated from the Stokes-Einstein equation, $R_h = RT/6\pi\eta DN$, where R = gas constant, T = absolute temperature, η = viscosity, N = Avogadro's number, and D = diffusion coefficient (our value). [b] Two determinations. [c] Value for fluorescein. [d] Single determination using the original, unfractionated F-dextran 3,000 or 10,000. [e] Value for dextran M_r of approximately 3600 (R_h = 1.20 nm).

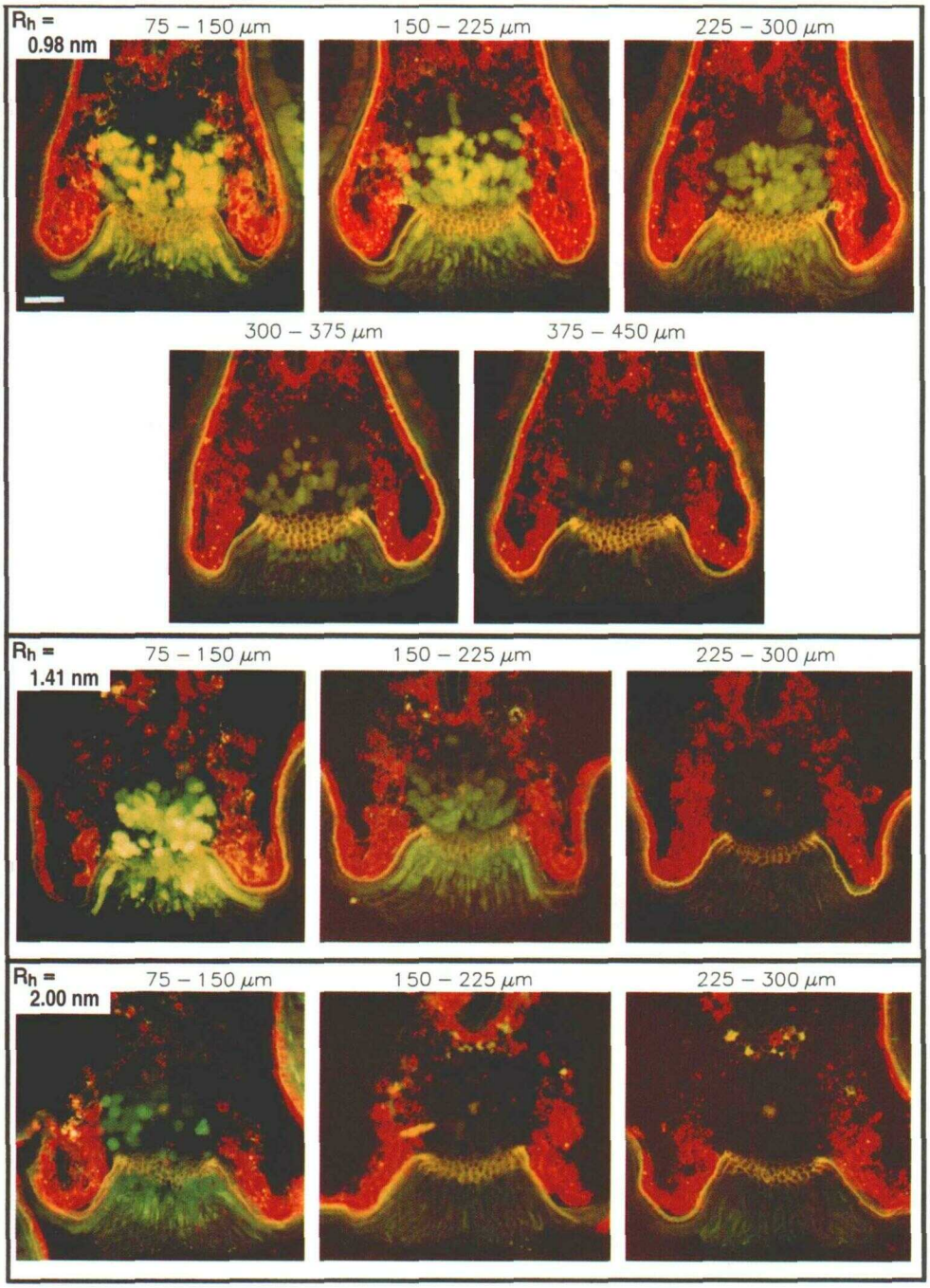

Figure 8. Longitudinal symplastic movement of F-dextrans, R_h = 0.98, 1.41, and 2.00 nm, along the grain axis. For each experiment, the grain was cut transversely and the cut surface was incubated for 2 min in 5 mM F-dextran at 0°C, followed by a wash in standard medium at room temperature for 28 min. Serial cross-sections, 75 μm thick, were cut with a vibrating microtome and washed at room temperature for 20 min in standard medium before viewing. For each sequence, the distance given is from the original cut surface. The first section of each sequence is not shown, since they were somewhat variable in thickness and showed appreciable nonspecific extracellular staining. Otherwise, except for less staining in the vascular parenchyma, they were basically similar in appearance to the 75- to 150-μm section in each sequence. The last section of the sequence for the 2.00-nm F-dextran (lower right micrograph) may be regarded as an unstained control for all these sequences. The chalaza and testa cuticle show a strong yellow autofluorescence. The bright red fluorescence is from chloroplasts, which are located entirely in the pericarp. Bar (upper left micrograph) = 100 μm.

showed at least some degree of symplastic mobility. The smallest F-dextran (R_h = 0.98 nm) moved along the symplast for at least 400 μm, traversing about 10 cells in 30 min. Mobility declined sharply as R_h increased, with 1.41- and 2.00-nm F-dextrans moving, very roughly, 250 and 180 μm, respectively. Similar experiments were run with 1.61- and 2.35-nm F-dextrans. Movement of the 1.61-nm F-dextran was intermediate between the 1.41- and 2.00-nm F-dextrans, whereas the 2.35-nm F-dextran was immobile.

The uptake patterns of representative F-dextran sizes are illustrated for one experiment in Figure 9. All sections were from the same grain. As much as possible, other conditions (fluorochrome concentration, uptake times, and photographic exposure times) were adjusted to allow direct comparisons between photomicrographs. The experiment was run eight times with basically similar results. The smallest F-dextran (R_h = 0.98 nm) showed strong fluorescence in the nucellus and in the vascular parenchyma between the xylem and chalaza, but not in the chalaza or vascular parenchyma external to the xylem. This pattern was frequently observed, even for smaller dyes (e.g. Figs. 2, 3, and 4), where the apparent lack of uptake more likely resulted from cell damage or from loss of absorbed dye, depending on the cells involved. Parenchyma cells outside the xylem become progressively longer between the xylem and pericarp (Fig. 5A), making them more susceptible to damage during sectioning. Chalazal cells, which absorb dye rapidly from solutions (Fig. 5), also seemed to retain their ability to exchange solutes longer, so they apparently lost more dye during postincubation washes.

The pattern of F-dextran uptake into much of the vascular parenchyma differed from that observed for symplastic movement (Fig. 8), at least for the larger F-dextrans. Uptake of F-dextrans larger than 1.16-nm R_h was localized largely in the nucellus, chalaza, and, in the vascular parenchyma, only in those cells immediately adjacent to the chalaza. This pattern showed little change with hydrodynamic radii from 1.16 to 2.00 nm. There was virtually no uptake of 2.35-nm F-dextran.

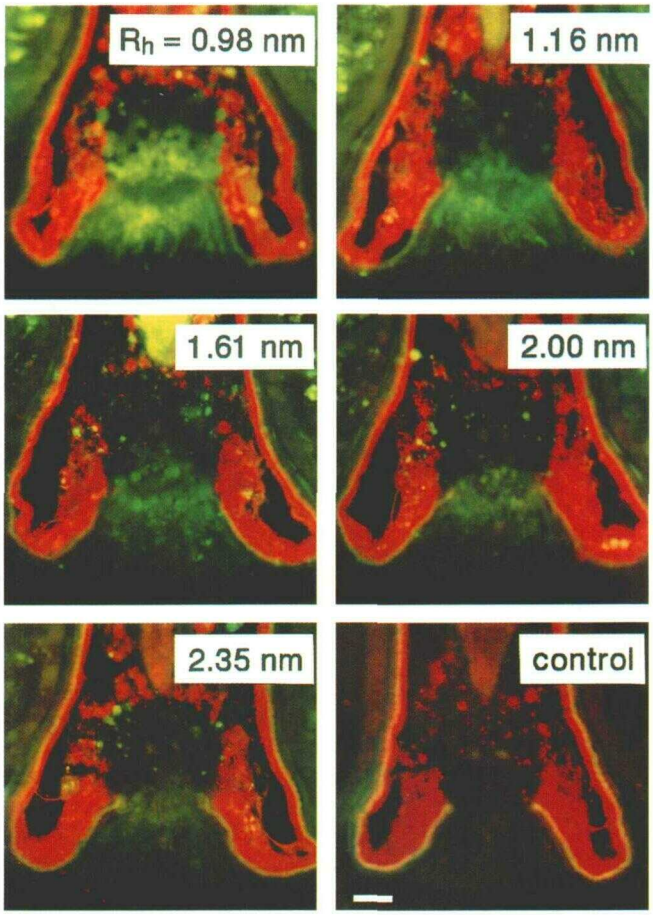

Figure 9. Uptake of size-fractionated F-dextrans by 100-μm fresh sections. All sections were cut from the same grain with a vibrating microtome. Incubation of F-dextran was at 0°C, followed by a 15-min wash in standard medium at room temperature. Fluorescence concentration was held constant in each solution (i.e. 0.5 mM for F-dextrans with R_h = 0.98–1.61 nm; 0.2 mM for 2.0-nm and larger F-dextrans), and proportionately longer incubation times were used for larger F-dextrans. Bar (lower right micrograph) = 100 μm.

DISCUSSION

On most major points, our observations confirm existing views of the nonvascular pathways for solute movement in the crease tissues of the wheat grain. Based on ultrastructural and histochemical investigations, Zee and O'Brien (1970b) concluded that the chalazal walls present a barrier to apoplastic solute movement. Additional evidence has been advanced for that view (e.g. Cochrane, 1983), but our observations provide the first direct experimental support. Using fluorescein as a symplastic tracer for phloem-imported assimilates, Cook and Oparka (1983) showed that it entered via the phloem and followed a symplastic pathway to the nucellus, from which it was released into the endosperm cavity. This last step, requiring permeation of the nucellar cell membranes, could not be confirmed with the more polar dyes used here. However, plant cell membranes can be quite permeable to fluorescein (Oparka, 1991), which probably accounts not only for its appearance in the endosperm cavity in Cook and Oparka's experiments, but for its initial movement into the sieve tubes. Our finding that CF can move readily from the nucellus to the vascular parenchyma, even against an intense flux of incoming assimilates, establishes the important fact that symplastic transport within the crease symplast is a bidirectional process. Clearly, this supports the view that diffusion provides a major, if not exclusive, basis for post-phloem assimilate movement across the crease. However, our observations are qualitative and do not exclude the possibility of at least some contribution from bulk flow.

Apoplastic movement across the crease was not blocked completely by the chalazal cell walls. Although movement was far slower than the rapid penetration of tracers into the nucellar walls, and even much slower than symplastic movement, fluorescent tracers applied to the nucellar surface consistently moved into the chalaza walls, or further, within a few hours. Presumably, the same path is available for limited movement of normally occurring solutes in the endosperm cavity. Since water molecules are much smaller, the pathway may have more significance for water movement. However,

the consistent presence of an appreciable water potential difference between the endosperm cavity and pericarp (about 0.3 MPa; Fisher, 1985; Fisher and Gifford, 1986) strongly implies that it must be a high-resistance pathway even for water movement.

The absorption of LYCH into nucellar cell cytoplasm from the endosperm cavity appeared to occur too slowly to have significant quantitative implications for the release of assimilates into the cavity. Although LYCH was located in the cytoplasm of the nucellar cells 0.5 to 1 h after cavity perfusion with LYCH, no symplastic movement of LYCH across the crease was observed. This contrasts with the rapid movement of CF when the cavity was perfused with CFDA. Perhaps LYCH absorption was sufficiently slow that it was being sequestered by subcellular compartmentation rather than transported. The mechanism of absorption was not addressed but, over the longer times involved, uptake may have occurred by endocytosis (Oparka, 1991) rather than passive movement.

The uptake of polar tracers into the intact cells of fresh-cut crease sections almost certainly occurred via unsealed plasmodesmata. The apparent uptake of small solutes via unsealed plasmodesmata in isolated plant tissues has been described previously by Burnell (1988) for bundle sheath strands from C_4 plants (SEL about 900 D) and by McCaskill et al. (1992) for glandular trichomes from peppermint leaves (SEL about 1800 D).

Dye uptake in the present experiments was very rapid and showed no evidence of metabolic dependency. Uptake did not occur everywhere from the apoplast, but was associated with cut cells, and, finally, it was sharply reduced by plasmolysis. An important aspect of fluorescent tracer uptake, for which there is no fully satisfactory explanation, is its retention after extended washes. In some cases this might be attributed to the progressive sealing of plasmodesmata or to subcellular redistribution into membrane-bound organelles. However, it seems questionable whether these processes could account for retention in the cold, where uptake and, it would seem, loss was not noticeably affected by preincubation at 0°C.

By itself, the SEL cannot be used to determine precisely the channel dimensions for intercellular movement. However, comparisons with the observations of Terry and Robards (1987) with *Abutilon* nectary trichomes clearly indicate that the channels must be appreciably larger than the 3-nm diameter estimated for *Abutilon*. This is readily evident from the easy mobility of 0.98-nm (R_h) F-dextran (M_r approximately 3000) in the vascular parenchyma (Figs. 8 and 9) and the uptake and symplastic movement in many cells of F-dextrans as large as 2.00-nm R_h. In *Abutilon*, F-Trp-Phe (M_r = 739, estimated R_h = 0.9 nm) was essentially immobile. Furthermore, a molecule's hydrodynamic radius, which is simply the radius of a sphere having an equivalent hydrodynamic drag coefficient, is not the most appropriate expression of molecular dimensions where entry of a polymeric molecule into a pore is concerned (Tanford, 1961; Luby-Phelps et al., 1986; Luby-Phelps, 1989, and refs. therein). This is especially true for an unbranched random coil, which the *Leuconostoc* dextrans used here approximate.

In the context of size exclusion from a pore, R_g is a more relevant measure of molecular size than is R_h. For these dextrans, an approximate relationship between the two is given by $R_g = 1.54\ R_h$ (the difference is probably somewhat greater [Tanford, 1961]; also, see Luby-Phelps et al. [1987] for a comparison of F-dextrans with Ficoll, which has more clearly defined molecular dimensions). Thus, the effective molecular diameter for the SEL in the crease tissues is about 6.2 nm for the nucellus, chalaza, and at least those cells of the vascular parenchyma near the chalaza. Estimates of the SEL in the remainder of the vascular parenchyma are less certain, given the differences in our observations of F-dextran uptake/retention versus symplastic movement there. On the grounds that cell-to-cell movement should be given more emphasis, a SEL of 6.2 nm may be likely. In any event, it is at least 3.6 nm and, at least in some cases, as large as 6.2 nm. Taken together, these considerations suggest intercellular channel diameters in most of the crease, except for the pericarp, of about 7.0 nm. This may also apply to the vascular parenchyma. However, even with a SEL there of only 3.6 nm the channel diameter must be at least 4.5 nm.

The effect of these larger-than-usual dimensions on the transport characteristics of individual channels is more than proportionate to their increased size. For diffusion, the combined effects of steric exclusion and frictional effects of the wall on solute movement (Paine and Scherr, 1975) would make a cylindrical pore 4.5 nm in diameter more than four times more conductive for Suc (R_h = 0.47 nm) than a 3-nm pore. A 7-nm pore would be almost 15 times more conductive. Since hydraulic conductivity should be proportional to the third-to-fourth power of the channel opening, depending on geometry, it would be increased by at least as much as for diffusive movement. Assuming that these changes have a proportionate effect on the cell-to-cell permeability coefficient, these relatively small, and probably microscopically undetectable, adjustments in plasmodesmatal structure may be sufficient to account for assimilate flux through the crease symplast.

Our observations are not yet sufficiently quantitative to fully evaluate the relative roles of diffusion and bulk flow in symplastic movement. Obviously, plasmodesmatal densities are needed to estimate total between-cell conductivities, but this applies equally to both types of movement. The ability of CF to diffuse against the movement of incoming assimilates supports the view that assimilate movement itself must be largely diffusive. Nonetheless, the "stairstep" distribution of diffusing PTS (Fig. 5) clearly indicates that, in this system as in others, cell-to-cell movement is substantially restricted in comparison to within-cell movement.

Concentration gradients that are invoked to drive diffusive movement must also be considered in evaluating cell-to-cell turgor differences and the bulk flow that would accompany those differences. Finally, in view of possible differences in channel size along the pathway, the relative contributions of diffusion and bulk flow to total transport could also vary along the path.

ACKNOWLEDGMENT

We thank Ms. Alexis Lansing for her capable and patient assistance in initiating several aspects of this work.

Received July 12, 1993; accepted September 20, 1993.
Copyright Clearance Center: 0032-0889/94/104/0017/11.

LITERATURE CITED

Anderson JL, Malone DM (1974) Mechanism of osmotic flow in porous membranes. Biophys J **14:** 957–982

Barclay GF, Peterson CA, Tyree MT (1982) Transport of fluorescein in trichomes of *Lycopersicon esculentum*. Can J Bot **60:** 397–402

Barlow EWR, Donovon GR, Lee JW (1983) Water relations and composition of wheat ears grown in liquid culture: effect on carbon and nitrogen. Aust J Plant Physiol **10:** 99–108

Burnell JN (1988) An enzymatic method for measuring the molecular weight exclusion limit of plasmodesmata of bundle sheath cells of C_4 Plants. J Exp Bot **39:** 1575–1580

Cochrane MP (1983) Morphology of the crease region in relation to assimilate uptake and water loss during caryopsis development in barley and wheat. Aust J Plant Physiol **10:** 473–491

Cook H, Oparka KJ (1983) Movement of fluorescein into isolated caryopses of wheat and barley. Plant Cell Environ **6:** 239–242

Finkelstein A (1987) Water Movement through Lipid Bilayers, Pores, and Plasma Membrane: Theory and Reality. John Wiley & Sons, New York

Fisher DB (1985) In situ measurement of plant water potentials by equilibration with microdroplets of polyethylene glycol 6000. Plant Physiol **79:** 270–273

Fisher DB, Frame JM (1987) A guide to the use of the exuding-stylet technique in phloem physiology. Planta **161:** 385–393

Fisher DB, Gifford RM (1986) Accumulation and conversion of sugars by developing wheat grains. VI. Gradients along the transport pathway from the peduncle to the endosperm cavity during grain filling. Plant Physiol **82:** 1024–1030

Fisher DB, Housley TL (1972) The retention of water-soluble compounds during freeze-substitution and microautoradiography. Plant Physiol **49:** 166–171

Fisher DB, Wang N (1993) A kinetic and microautoradiographic analysis of [^{14}C]sucrose import by developing wheat grains. Plant Physiol **101:** 391–398

Goodwin PB, Shepherd V, Erwee MG (1990) Compartmentation of fluorescent tracers injected into the epidermal cells of *Egeria densa* leaves. Planta **181:** 129–136

Granath KA, Kvist BE (1967) Molecular weight distribution analysis by gel chromatography in Sephadex. J Chromatogr **28:** 69–81

Grimes HD, Slay RM, Hodges TK (1988) Plant plasma membrane proteins. II. Biotinylation of *Daucus carota* protoplasts and detection of plasma membrane polypeptides after SDS-PAGE. Plant Physiol **88:** 444–449

Jenner CF (1974) Factors in the grain regulating the accumulation of starch. *In* RL Bieleski, AR Ferguson, MM Cresswell, eds, Mechanisms of Regulation of Plant Growth. Bulletin 12, The Royal Society of New Zealand, Wellington, pp 901–908

Jenner CF (1985a) Control of the accumulation of starch and protein in cereal grains. *In* B Jeffcoat, AF Hawkins, AD Stead, eds, Regulation of Sources and Sinks in Crop Plants. British Plant Growth Regulator Group, Long Ashton, UK, pp 195–210

Jenner CF (1985b) Transport of tritiated water and ^{14}C-labeled assimilate into grains of wheat. III. Diffusion of THO through the stalk. Aust J Plant Physiol **12:** 595–608

Lide DR (1990) CRC Handbook of Chemistry and Physics, Ed 71. CRC Press, Boca Raton, FL

Luby-Phelps K (1989) Preparation of fluorescently labeled dextrans and Ficolls. *In* YL Wang, DL Taylor, eds, Fluorescence Microscopy of Living Cells in Culture. Part A: Fluorescent Analogs, Labeling Cells, and Basic Microscopy. Academic Press, San Diego, CA, pp 59–73

Luby-Phelps K, Castle PE, Taylor DL, Lanni F (1987) Hindered diffusion of inert tracer particles in the cytoplasm of mouse 3T3 cells. Proc Natl Acad Sci USA **84:** 4910–4913

Luby-Phelps K, Taylor DL, Lanni F (1986) Probing the structure of cytoplasm. J Cell Biol **102:** 2015–2021

McCaskill D, Gershenzon J, Croteau R (1992) Morphology and monoterpene biosynthetic capacities of secretory cell clusters isolated from glandular trichomes of peppermint (*Mentha piperita* L.). Planta **187:** 445–454

Oparka KJ (1991) Uptake and compartmentation of fluorescent probes by plant cells. J Exp Bot **42:** 565–579

Paine PL, Moore LC, Horowitz SB (1975) Nuclear envelope permeability. Nature **254:** 109–114

Paine PL, Scherr P (1975) Drag coefficients for the movement of rigid spheres through liquid-filled cylindrical pores. Biophys J **15:** 1087–1091

Porter GA, Knievel DP, Shannon JC (1985) Sugar efflux from maize (*Zea mays* L.) pedicel tissues. Plant Physiol **77:** 524–531

Schantz EJ, Lauffer MA (1962) Diffusion measurement in agar gel. Biochemistry **1:** 658–663

Sofield I, Wardlaw IF, Evans LT, Zee SY (1977) Nitrogen, phosphorus and water contents during grain development and maturation in wheat. Aust J Plant Physiol **4:** 799–810

Tanford C (1961) Physical Chemistry of Macromolecules. John Wiley & Sons, New York

Terry BR, Robards AW (1987) Hydrodynamic radius alone governs the mobility of molecules through plasmodesmata. Planta **171:** 145–157

Tucker JE, Mauzerall D, Tucker EB (1989) Symplastic transport of carboxyfluorescein in staminal hairs of *Setcreasea purpurea* is diffusive and includes loss to the vacuole. Plant Physiol **90:** 1143–1147

Wang N, Fisher DB (1994) Monitoring phloem unloading and post-phloem transport by microperfusion of developing wheat grains. Plant Physiol **104:** 7–16

Wolswinkel P (1992) Transport nutrients into developing seeds: a review of physiological mechanisms. Seed Sci Res **2:** 59–73

Zee SY, O'Brien TP (1970a) A special type of tracheary element associated with "xylem discontinuity" in the floral axis of wheat. Aust J Biol Sci **23:** 783–791

Zee SY, O'Brien TP (1970b) Studies on the ontogeny of the pigment strand in the caryopsis of wheat. Aust J Biol Sci **23:** 1153–1171